BIOCHEMISTRY
including biophysical chemistry & molecular biology

Article

pubs.acs.org/biochemistry

Obtaining Optical Purity for Product Diols in Enzyme-Catalyzed Epoxide Hydrolysis: Contributions from Changes in both Enantio- and Regioselectivity

Åsa Janfalk Carlsson, Paul Bauer, Huan Ma, and Mikael Widersten*

Department of Chemistry-BMC, Uppsala University, Box 576, SE-751 23 Uppsala, Sweden

Supporting Information

ABSTRACT: Enzyme variants of the plant epoxide hydrolase StEH1 displaying improved stereoselectivities in the catalyzed hydrolysis of (2,3-epoxypropyl)benzene were generated by directed evolution. The evolution was driven by iterative saturation mutagenesis in combination with enzyme activity screenings where product chirality was the decisive selection criterion. Analysis of the underlying causes of the increased diol product ratios revealed two major contributing factors: increased enantioselectivity for the corresponding epoxide enantiomer(s) and, in some cases, a concomitant change in regioselectivity in the catalyzed epoxide ring-opening half-reaction. Thus, variant enzymes that catalyzed the hydrolysis of racemic (2,3-epoxypropyl)benzene into the *R*-diol product in an enantioconvergent manner were isolated.

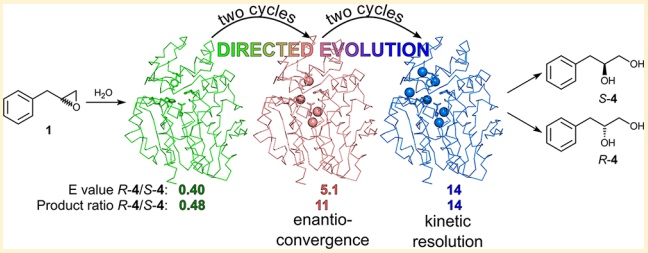

The catalytic powers of enzymes present great potentials as replacements or complements to presently dominating approaches in organic synthesis. The inherently asymmetric nature of enzymes' active sites facilitates specific and efficient reactions involving chiral reactants and intermediates. Still, adoption of enzymes in synthetic regimes is slow, which may be attributed to different issues. Enzymes are, by evolution of their biological roles, generally too specific in their substrate acceptance to become useful synthetic tools in reactions involving a wider structural range of related compounds. Enzymes are, with exceptions, prone to denature in organic solvents, which prevents their inclusion in presently used synthetic protocols. The development of methodologies affording re-engineering of both functional and physicochemical properties of enzymes, however, shows promise that most, if not all, of these issues can be addressed.[1−8]

We have set out to design multistep reactions catalyzed solely by enzymes involving chiral starting compounds that are transformed into stereochemically defined products. Naturally occurring enzymes are identified on the basis of catalyzed chemistry rather than substrate selectivity and are re-engineered through the process of directed evolution[9−13] into potential biocatalysts that display desired catalytic functions and substrate selectivities. The starting reactants are chiral epoxides that are hydrolyzed into likewise chiral vicinal diols (Scheme 1) that can be further derivatized in subsequent reaction steps. Both the epoxides and the product diols are important precursors in the synthesis of asymmetric compounds, and the possibility of producing these molecules in optically pure form is therefore of interest.[14]

The enzyme-catalyzed reactions found for naturally occurring epoxide hydrolases are S_N2-type reactions in which the epoxide ring is opened either by a base-activated water molecule, such as in the limonene epoxide hydrolyzing enzyme, or by an enzyme-contributed carboxylate, thereby forming a covalent alkyl−enzyme intermediate.[15−18] The latter mechanism is present in the α/β-hydrolase-type enzymes,[19−22] with the ring opening being facilitated by enzyme-provided acids, a Tyr pair.[23,24] Our group is using the potato epoxide hydrolase StEH1[25,26] as the starting scaffold for engineering new epoxide hydrolase enzymes that can be applied as biocatalysts for chiral epoxide ring-opening reactions.[27] StEH1 differs in active-site structure and substrate selectivity from a previously engineered *Aspergillus niger* epoxide hydrolase.[22,28−30] The substrate binding site in StEH1 is larger, thus broadening the substrate scope of the wild-type enzyme compared to that of the *A. niger* isoenzyme.

Scheme 1. Hydrolysis of a Chiral Epoxide into Vicinal Diols

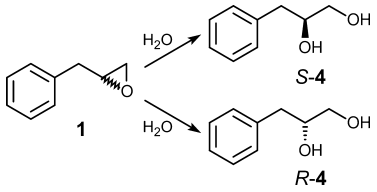

The intrinsic reactivities of the oxirane carbons in a ring-opening reaction with an electron rich nucleophile (such as a carboxylate) depend on the additional substituents of the epoxide. Since the transition state involves a partially positively

Received: June 11, 2012
Revised: August 23, 2012
Published: August 29, 2012

charged carbon, an electron-donating group, such as phenyl, will promote addition of the nucleophile at the substituted carbon. Consequently, electron-withdrawing groups steer nucleophilic attack toward the other epoxide carbon.[31] In epoxides without electron-donating or -withdrawing substituents, other factors like steric hindrance will become more important. In enzyme-catalyzed ring opening, however, these guiding principles of expected product outcome are overturned and other restraints, such as active-site structure, will influence regioselectivity. This is well illustrated by StEH1-catalyzed hydrolysis of styrene oxide [**2** (Chart 1)] and *trans*-2-methylstyrene oxide (**3**). The enzyme-afforded ring opening of *S*-**2** does involve nucleophilic attack at the (expected) benzylic carbon but preferentially at the least hindered carbon with the *R*-enantiomer.[32] A similar behavior has been observed in the catalyzed hydrolysis of **3** where the *S*,*S*-enantiomer is exclusively attacked at the benzylic carbon, whereas the regiopreference in the hydrolysis of *R*,*R*-**3** varies with changes in temperature and pH.[33] These findings suggest that regioselectivity in StEH1 catalysis may be amenable to manipulation by directed protein evolution.

Chart 1. Epoxide Substrates

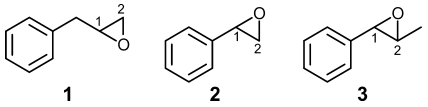

The apparent structural requirements of the catalyzed reaction are (i) complementarity of the epoxide and the active-site compartment and (ii) correct spatial orientation of the epoxide with respect to both the catalytic acid(s) (two Tyr residues) and the nucleophilic Asp (see Figure 1 for the working model of the catalytic mechanism of StEH1). The hydrolytic step of the catalytic cycle, which generally is the rate-limiting step, is expected to contribute to a lesser degree to deciding product outcome but rather influence the overall reaction rate.[24,28,34] Therefore, it is possible to make naive assumptions about product outcomes from docking experiments or more elaborate calculations.[35−38] The detailed understanding is, however, unclear, which is unsatisfactory from a perspective of manipulating properties such as stereoselectivity by rational approaches guided by first principles.

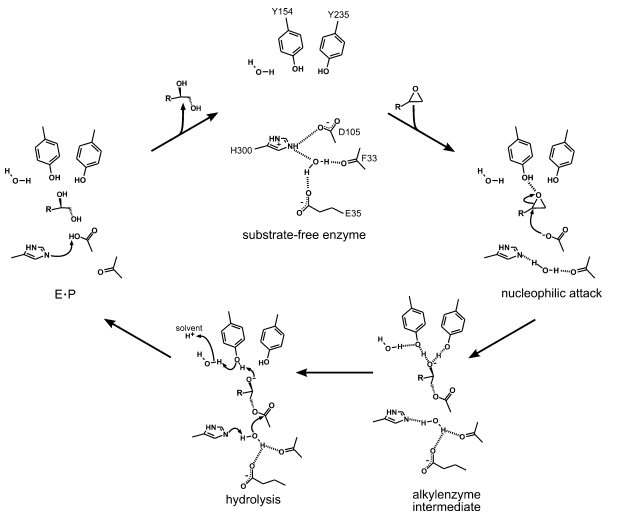

Figure 1. Current working model of the catalytic mechanism of StEH1. The nucleophilic carboxylate of Asp105 reacts with one of the electrophilic epoxide carbons. The subsequent ring opening is catalyzed by hydrogen bonding of the leaving group oxyanion to the phenols of Tyr154 and Tyr235. The so-formed covalent alkyl−enzyme intermediate is hydrolyzed in the general base (His300)-catalyzed half-reaction to yield the diol product.

(2,3-Epoxypropyl)benzene (**1**) will, upon catalyzed hydrolysis, form either the *R*-**4** or the *S*-**4** diol. The outcome depends both on the enantiopreference of the enzyme for the epoxide substrate and on the regioselectivity of the attack. Wild-type StEH1 catalyzes the hydrolysis in a regiospecific manner in which the enzyme-contributed nucleophile (D105 carboxylate) attacks the epoxide at the (expected) least hindered nonchiral carbon 2 (Chart 1). The catalyzed hydrolysis causes retention of configuration, and the resulting diol products therefore inherit the stereochemistry of the reactant epoxides. The enantioselectivity of StEH1 with racemic **1** is low with a 2.5-fold preference for hydrolysis of *S*-**1** as compared to the *R*-enantiomer.[27]

In this work, we set out to modify the stereoselectivity of the StEH1-catalyzed reaction with **1** to generate enzyme variants yielding an enriched enantiomer excess of the resulting chiral product diols. The aim was set without favoring alterations in enantio- or regioselectivities, because either, or in combination, can potentially generate the same result of improved product optical purity. As discussed above, lacking the necessary understanding of the prerequisites for steering selectivity in substrate acceptance and regioselectivity in nucleophilic attack, we applied the semirational iterative saturation mutagenesis (ISM) approach originally introduced by M. Reetz.[39,40] This strategy has proven to be efficient in producing enzyme variants with improved desired properties.[41−45] The approach relies on subdividing the active site into groups of amino acid residues deemed to affect the targeted property. In this study, the StEH1 active site was divided into five subsites, A−E (Figure 2), maintaining one (A, F33), two (B, W106 and L109; C*, L145 and I155; D, I180 and F189; and E, L266 and V267), or three (C, V141, L145, and I155) residues. Applying a codon-limited mutagenesis regime (NDT) further served to generate mutant libraries of manageable sizes. The decrease in the possible structural diversity, from 20^n to 12^n variants in the NDT mutated libraries, is a reasonable trade-off because the hit rate has been shown to be comparable while the effort in library constructions and screening becomes greatly reduced.[46] The approach allowed for isolation of StEH1 variants displaying distinct stereoselectivities with epoxide **1** that also had acquired altered selectivities with the related epoxides **2** and **3**. These substrates were included because of both their structural similarities with epoxide **1** and their relevance in synthetic chemistry. The aim was to see patterns and potential similarities, concerning, e.g., enantio- and regioselectivity, between the various substrates and enzyme variants.

MATERIALS AND METHODS

Chemicals and Reagents. All chemicals used were of the highest purity commercially available.

Construction of Enzyme Libraries. The sites used for mutations were A (F33), B (W106 and L109), C (V141, L145, and I155), and D (I180 and F189), with the addition of C* (L145 and I155) and E (L266 and V267). For the *R*-specific variants, the previously generated quadruple mutant R-C1B1[27]

dx.doi.org/10.1021/bi3007725 | *Biochemistry* 2012, 51, 7627−7637

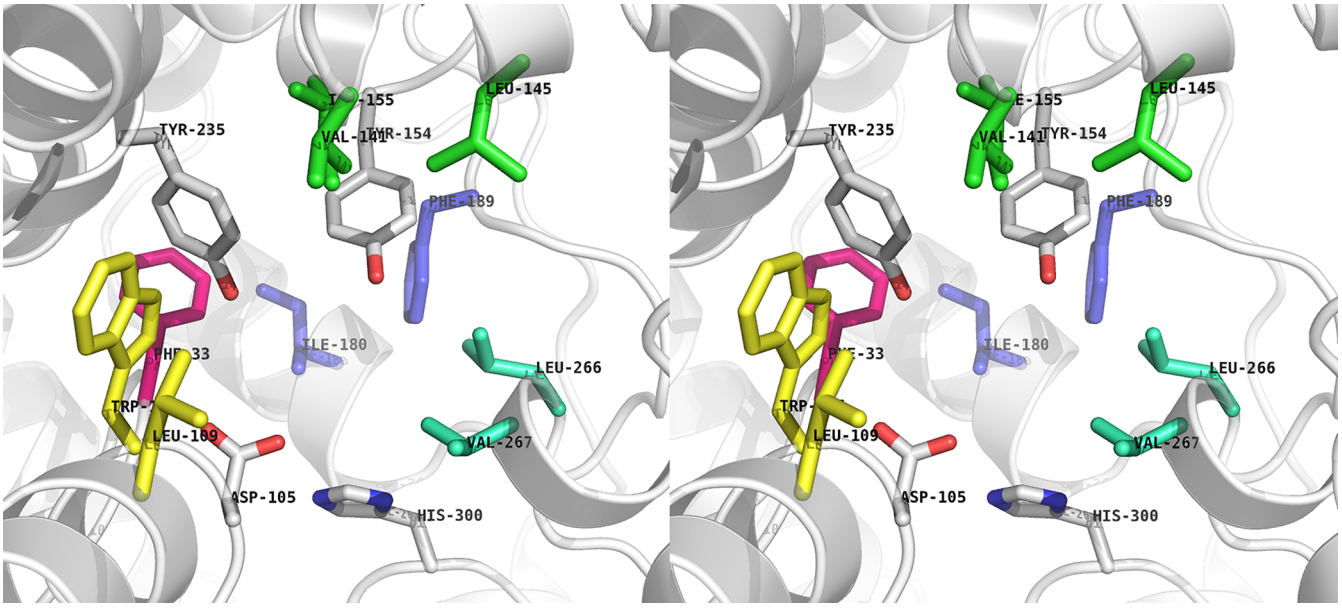

Figure 2. Stereo image of the active site of StEH1. Side chains of residues included in the iterative mutagenesis are shown as colored sticks: library A (F33) in magenta, library B (W106 and L109) in yellow, library C (V141, L145, and I155) in green, library D (I180 and F189) in blue, and library E (L266 and V267) in cyan. Catalytic residues are shown as white sticks. Library C* does not include V141 as an altered site. Image created with PyMol (http://www.pymol.org) applying the atomic coordinates of Protein Data Bank entry 2CJP.[28]

was used as a template for further mutations at the A and D sites. In accordance with the idea of the ISM approach,[6,39] the top candidate from the D library (R-C1B1D33) was subsequently used as a template for the E library. Similarly, the *S*-specific variants were constructed using the wild-type StEH1 cDNA together with primers for the A and B libraries where the top candidate from the B library (S-B17) then was used as the template for both the C* and D libraries. All primers used are listed in Table SI1 of the Supporting Information, in which a degenerate NDT codon set, leading to 12 possible amino acids, was used for each mutation site. The mutants were constructed using nested polymerase chain reaction (PCR) except for the A library, using QuikChange, and the D library, using normal PCR. Each library was transformed by electroporation into *Escherichia coli* XL-1 Blue cells carrying the pREP4 GroEL/ES vector,[47] allowing for overexpression of chaperonins. Colonies were selected on LB-agar plates, supplemented with 100 μg/mL ampicillin and 30 μg/mL kanamycin, and the qualities of the constructed libraries were verified by sequencing at least 20 randomly picked clones.

Cultivation and Expression of Libraries. Cells were grown in 96-well microtiter plates. Single colonies were inoculated into wells containing 350 μL of 2TY (16 g/L tryptone, 10 g/L yeast extract, and 5 g/L NaCl) with 100 μg/mL ampicillin and 30 μg/mL kanamycin added. Culture wells were covered with gas permeable film and incubated for 18 h at 30 °C and 175 rpm. The overnight culture (25 μL) was reinoculated into 325 μL of 2TY with 50 μg/mL ampicillin and 15 μg/mL kanamycin. After incubation for 5 h, expression of StEH1 protein variants together with GroEL/ES chaperonins was induced by addition of isopropyl β-D-thiogalactopyranoside (IPTG) (final concentration of 1 mM). Expression was allowed for 18 h, and cells were harvested by centrifugation. Cells were lysed by addition of 25 μL of Bacterial Protein Extraction Reagent (B-PER), with protease inhibitor added, to each well. The cell pellets were resuspended by being vortexed and then incubated for 40 min at room temperature. To increase the volume, 75 μL of 0.1 M sodium phosphate buffer (pH 7.0) was added before the cell debris was centrifuged for 1 h at 4 °C and 3500 rpm. The lysate was stored cold until it was used.

Screening of Libraries. The screening reactions were performed in duplicate for *R*- and *S*-**1**, where 25 μL of lysate from each well was transferred to each of four different flat-bottom plates. To each well was added 25 μL of 10 mM **1** [dissolved in 0.1 M sodium phosphate buffer (pH 7.0) with 10% (v/v) DMSO]. The reaction mixtures were incubated for 10−20 min, depending on the activity of the enzyme variants, at 30 °C and 200 rpm. To assay the remaining epoxide, a colorimetric method as described by Agarwal[48] was applied. Twenty-five microliters of 100 mM 4-(4-nitrobenzyl)pyridine [dissolved in an 80:20 (v/v) glycol/ethanol mixture] was added. The reaction between nitrobenzyl pyridine and remaining epoxide was allowed for 20 min at 80 °C and 200 rpm before being stopped by addition of 50 μL of ethanol. After addition of 25 μL of 1 M K_2CO_3, color, indicative of nonhydrolyzed epoxide, appeared. To estimate epoxide hydrolase activities in each well, the absorbances at 570 nm were measured using a microtiter plate reader. The apparent hydrolase activities were used to identify potential hits. The corresponding StEH1 cDNAs were sequenced to identify the inserted mutations. Unique variants were subsequently verified as hits by a repeated round of activity measurement.

Protein Expression and Purification of Hits. The expression plasmid encoding a selected variant was transformed into *E. coli* XL-1 Blue cells, carrying the pREP4 GroEL/ES plasmid. A single colony was inoculated into 5 mL of 2TY with 100 μg/mL ampicillin and 30 μg/mL kanamycin and grown overnight at 30 °C and 200 rpm. The overnight culture was diluted in 0.5 L of 2TY medium containing 50 μg/mL ampicillin and 15 μg/mL kanamycin and grown at 30 °C and 200 rpm. When the OD_{600} reached 0.4, protein expression of both the StEH1 variants and the chaperonins was induced by the addition of IPTG (final concentration of 1 mM). Expression was allowed for 18 h at 30 °C and 200 rpm, and

dx.doi.org/10.1021/bi3007725 | *Biochemistry* 2012, 51, 7627−7637

cells were harvested by centrifugation. The cell pellet was stored at −80 °C until it was further treated.

Protein purification was performed in a batch manner in which all the purification steps were conducted under slow agitation at 4 °C. First, the pellet from a 0.5 L culture was resuspended in 20 mL of binding buffer [0.1 M sodium phosphate, 0.5 M NaCl, and 20 mM imidazole (pH 7.4)] with added DNaseI and protease inhibitor. Cells were lysed using a Constant Systems Cell disruptor at 1.7 kPa, and the lysate was centrifuged for 1 h at 30000*g*. The supernatant was transferred to a 50 mL conical tube containing 1−2 mL of chelating resin, preloaded with Ni^{2+}. The mixture was incubated for 30 min before being centrifuged for 5 min at 700*g*. The supernatant was discarded, and 20 mL of washing buffer [0.1 M sodium phosphate, 0.5 M NaCl, and 0.1 M imidazole (pH 7.4)] was added. After incubation for 10 min, the resin was centrifuged at 700*g* and the supernatant was discarded. This washing step was then repeated. The protein was eluted by resuspending the resin in 2.5 mL of elution buffer [0.1 M sodium phosphate, 0.5 M NaCl, and 0.3 M imidazole (pH 7.4)]. After incubation for 5 min, the resin was centrifuged at 800*g* for 5 min. As a last step, the supernatant was transferred to a PD-10 desalting column, equilibrated with 0.1 M sodium phosphate buffer (pH 7.4), and eluted with 3.5 mL of equilibration buffer. The elution step was repeated, whereafter purity was confirmed by sodium dodecyl sulfate−polyacrylamide gel electrophoresis. Purified enzyme variants were stable for several weeks when stored in the cold. Protein concentrations were determined by measuring UV absorption at 280 nm, using an extinction coefficient (ε) based on the value for wild-type StEH1,[26] corrected by the following formula:

$$\varepsilon = \varepsilon_{WT} + \Delta Trp \times 5500 + \Delta Tyr \times 1490 + \Delta Cys \times 125$$

Enantiomeric Excess of Diol Product. The substrate *rac*-**1** was added, together with acetonitrile [3% (v/v)], to 0.1 M sodium phosphate buffer (pH 7.0) to a concentration of 30.4 mM. The reactions were assayed in triplicate at 30 °C. Enzyme (0.5 μM) was added to start the reactions, which were followed by the removal of aliquots at regular time points between 0 and 60 min. The reactions were stopped by addition of methanol to a final concentration of 50% (v/v). Solvent was evaporated for 5 h in a vacuum centrifuge at 800 rpm and the pellet resuspended in a hexane/2-propanol mixture [80:20 (v/v)]. The relative amounts of each *R*- and *S*-**4** were analyzed by chiral high-performance liquid chromatography (HPLC) [Daicel Chiralpak AS-H (250 mm × 4.6 mm inside diameter)] using a hexane/2-propanol mixture [90:10 (v/v)] as a mobile phase. The system used a LC 20AD solvent delivery module (Shimadzu, Tokyo, Japan), a Shimadzu SIL-10AF autosampler, and a Shimadzu SPDM20A photometric unit with the flow rate set at 0.5 mL/min. The retention times were 23 and 28 min for *S*-**4** and *R*-**4**, respectively.

Kinetic Characterization. Steady-state kinetic parameters for substrates **2** and **3** were determined by measuring initial rates of epoxide consumption as a decrease in absorbance at 225 nm (ε values of −2.75 and −4.3 mM^{-1} cm^{-1} for **2** and **3**, respectively). Reaction mixtures, containing pure enantiomers of each substrate (final concentrations of 0.016−0.7 mM) dissolved in 0.1 M sodium phosphate buffer (pH 7.5) with acetonitrile [1% (v/v)] added, were incubated at 30 °C. Reactions were started by addition of 0.5−1 μM enzyme.

For the reactions using epoxide **1** as the substrate, a protocol adapted from ref 27 was used. The substrate (final concentrations ranging from 0.12 to 4.5 mM) was added to 0.1 M sodium phosphate buffer (pH 7.0) and acetonitrile [3% (v/v)]. The reaction mixtures were incubated at 30 °C, before the enzyme (final concentrations of 50−200 nM) was added. Reactions were performed in triplicate with aliquots taken out after 0.5, 1.5, 2.5, and 3.5 min. The reactions were stopped by addition of methanol (with added phenylethyl alcohol as the internal standard) to a final concentration of 50% (v/v). Samples were kept on ice from this point or stored at −20 °C until they were analyzed. Samples were analyzed using reverse phase HPLC with a mixture of 0.1 M sodium phosphate buffer (pH 3.0) and methanol [63:37 (v/v)] as the mobile phase on a Supelco Ascentis C18 column (250 mm × 4.6 mm, 5 μm). The flow rate was set to 0.8 mL/min with the rest of the system being built up as previously described. Peaks were detected at 220 nm with approximate retention times of 15 and 50 min for diol **4** and epoxide **1**, respectively.

Analysis of Regioselectivity. To identify the peaks for *R*-**4** and *S*-**4** in the HPLC chromatogram, ^{13}C NMR was used to analyze the product of a reaction catalyzed by StEH1, proven to have a strict regioselectivity with **1**. Enzyme (1 μM) was mixed with 25 mM *S*-**1** in 0.1 M sodium phosphate buffer [1:1 (v/v) $H_2{}^{16}O/H_2{}^{18}O$] (pH 7.0). For the solubility of the epoxide, acetonitrile was added to a final concentration of 3% (v/v). Substrate was added in 2 μL aliquots over time to further increase solubility. The reaction mixture was incubated for 16 h at 30 °C and 400 rpm, whereafter product formation was confirmed by reverse phase HPLC. Prior to NMR analysis, D_2O (final concentration of 10%) was added to the sample. NMR spectra were recorded at 500 MHz (^1H) and 125.7 MHz (^{13}C) on a Varian Inova spectrometer. For the ^{18}O-labeled compounds, ^{13}C NMR spectra were recorded over a spectral range of 30 kHz, using an acquisition time of 1.3 s, a relaxation delay of 3 s, and a pulse flip angle of 44°. A total of 14200 transients (total experiment duration of 17 h) were acquired, for a final signal:noise ratio of 40−70. Data were processed with zero filling to 524288 points and Gaussian apodization. The result allowed assignment of the respective diol peaks obtained after chiral HPLC, as described below (Figure SI1 of the Supporting Information).

To determine the regioselectivity of the purified enzymes, reactions with 10−15 mM enantiopure (>98%) substrates **1**−**3** were performed overnight at 30 °C with slow agitation in a 500 μL total reaction volume using 0.5 μM enzyme and 3% (v/v) acetonitrile in 0.1 M sodium phosphate buffer (pH 7.0). After incubation, 500 μL of methanol was added to stop the reactions, whereafter the solvents were evaporated as previously described. The precipitate was resuspended in an 80:20 (v/v) hexane/2-propanol mixture and kept at −20 °C until further analysis. Samples were vortexed and centrifuged for 5 min at 13000 rpm to remove insoluble debris before being analyzed by chiral HPLC. The diol products formed from epoxides **2** and **3** were detected by measuring the absorbance at 225 nm, whereas the hydrolysis products of **1** were detected at 220 nm.

Protein Sequence Alignments. The StEH1 sequence was used as query in a protein BLAST[49] search of the plant subset of the UniProtKB database using the online tool at http://www.uniprot.org. Hit sequences of varying degrees of sequence identity (scores of 300−550) were collected and submitted to a ClustalW[50] multiple-sequence alignment.

RESULTS

Enzyme Library Constructions and Screening. *Increase in the Enantiomer Excess of R-4 from Racemic 1.* A previous initial study generated an enzyme variant,[27] hereafter called R-C1B1 (Table 1), which was chosen to template further mutagenesis at subsites A and D (Figure 2). The constructed protein expression libraries R-C1B1A and R-C1B1D maintained 12 and 144 members, respectively. To ensure a full coverage of potential protein variants, well above a theoretical coverage of >95%, all libraries were oversampled at least 3-fold when screening for epoxide hydrolase activity with **1** (Table 1).

Table 1. Library Data

template	library	mutated residues	library size	no. of screened clones	no. of hits
R-C1B1	A	F33	12	168	2
R-C1B1	D	I180, F189	144	504	42
R-C1B1D33	E	L266, V267	144	504	8
StEH1 wt	A	F33	12	168	13
StEH1 wt	B	W106, L109	144	504	17
S-B17	C*	L145, I155	144	504	19
S-B17	D	I180, F189	144	504	18

Two hits were isolated from the R-C1B1A library, which both had retained wild-type F33 through silent mutations (TTT in the NDT codon set) (Table SI2 of the Supporting Information). From the R-C1B1D library, 42 hits were collected and sequenced. A subset of these clones, chosen on the basis of apparent enzyme activity in the screening assay, were purified and analyzed via chiral HPLC to map the abilities to afford an increased *R*-**4**:*S*-**4** ratio. The variant displaying the highest ratio compared to the parent was R-C1B1D33 (Figure 3 and Table 2). The selection process was repeated with R-C1B1D33 as the template for mutagenesis at the E site. From this R-C1B1D33E library, eight clones were isolated (Table SI2 of the Supporting Information) where the variants displaying the highest enantiomer ratio of *R*-**4** were R-C1B1D33E3 and -E6, L266F and L266G, respectively (Figure 3).

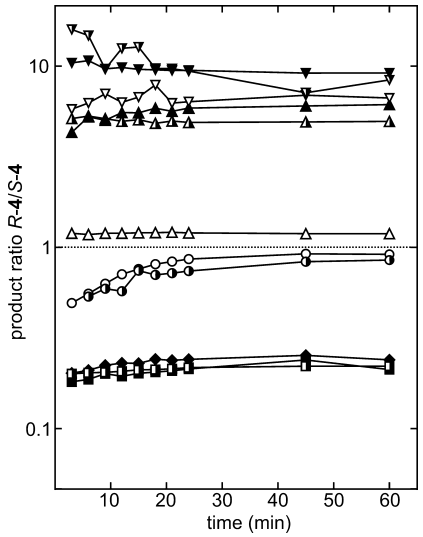

Figure 3. Ratios of diol products *R*-**4** and *S*-**4** over time after 0.5 μM enzyme-catalyzed hydrolysis of 30.4 mM racemic **1**: wild-type StEH1 (○), R-C1 (△), R-C1B1-K141V (◭), R-C1B1 (▲), R-C1B1D33 (▽), R-C1B1D33E3 (▽), R-C1B1D33E6 (▼) S-A8 (◑), S-B17 (◆), S-B17C*10 (■), and S-B17D14 (◨). Data points are mean values of three independent measurements.

Increase in the Enantiomer Excess of S-4 from Racemic 1. Libraries S-A and S-B were constructed and analyzed, following the same procedure described above, using wild-type StEH1 cDNA as the template. From the S-A library, 13 hits were isolated and sequenced (Table SI2 of the Supporting Information). The F33C and F33Y mutants were analyzed for their abilities to increase the enantiomer excess of *S*-**4** with only F33C displaying a slight improvement (Figure 3). From the S-B library, where 17 hits were sequenced, a variant (S-B17) showing a more pronounced increase was found (Table 2 and Figure 3). S-B17 was therefore subsequently used to template mutagenesis at the C* or D site. From these respective libraries, variants S-B17C*10 and S-B17D14 were identified as catalyzing the formation of *S*-**4** with a slightly increased enantiomer excess compared to that of the parent S-B17 variant (Figure 3).

Primary Structures of Selected Variants. In general, the hydrophobic nature of the active-site residues targeted for ISM was retained also in the isolated variants, and the observed replacements, with few exceptions, can be considered conservative (Table SI2 of the Supporting Information). Among the variants displaying increased product ratios of the respective diol enantiomers, all substitutions except V141K and L145R retained the nonpolar character of the initial residues (Table 2). The L145R replacement in S-B17C*10, however, appears to represent a phenotypically silent mutation because it was functionally indistinguishable from the related variant S-B17C*9 (L145H) in the reactions with epoxides **2** and **3** (Table SI3 of the Supporting Information).

In the S-B library selection, the aromatic character of the original Trp residue was conserved by Tyr or Phe substitutions in 13 of 17 selected hits (Table SI2 of the Supporting Information).

Catalytic Activities. The steady state kinetic data are presented in Table SI3 of the Supporting Information and are described here.

R-4 Selected Variants. A desired property of these mutants was an acquired ability to catalyze the production of *R*-**4** with refined optical purity, as compared to that of the parental StEH1 enzyme. Therefore, with retained regioselectivity, an increased ratio of the catalytic efficiencies between *R*-**1** and *S*-**1** was the expected outcome for the variants displaying an increased enantiomer excess of *R*-**4**. This was also the general trend; the k_{cat}/K_M for *S*-**1** decreased, from 42 to <1 s^{-1} mM^{-1}, during the iterations of mutagenesis and selection, while the activity with the *R*-enantiomer decreased less, from 17 to 12 s^{-1} mM^{-1} in the furthest evolved mutant R-C1B1D33E3 (Table SI3 of the Supporting Information). The resulting *E* values of 3 for variant R-C1B1D33 (an 8-fold increase compared to that of the wild-type enzyme) and 14 for mutant R-C1B1D33E3, however, did not solely explain the improvements that were observed in the *R*-**4**:*S*-**4** ratios. A general observation was that the individual parameters k_{cat} and K_M were affected in the direction of maintained turnover of *R*-**1** and increased values of K_M for both substrate enantiomers with the exception of R-C1B1D33E3, which maintained a comparably low $K_M^{R\text{-}1}$ (Table SI3 of the Supporting Information).

The selected variants were also analyzed for their acquired catalytic functions toward related epoxides **2** and **3**. With styrene oxide (**2**), the most dramatic effect was the increase in enantioselectivity for *S*-**2**, from 69 to 5800 for R-C1B1D33. The effect can be attributed to an 80-fold decrease in the

dx.doi.org/10.1021/bi3007725 | *Biochemistry* 2012, 51, 7627−7637

Table 2. Primary Structures of Selected Mutants

	library A	library B		library C			library D		library E	
		106	109	141	145	155	180	189	266	267
wild-type	F	W	L	V	L	I	I	F	L	V
R-C1				K	°[a]	V				
R-C1B1		L	Y	K	°	V				
R-C1B1D33		L	Y	K	°	V	°	L		
R-C1B1D33E3		L	Y	K	°	V	°	L	F	°
R-C1B1D33E6		L	Y	K	°	V	°	L	G	°

	library A	library B		library C*		library D	
	33	106	109	145	155	180	189
S-A8	C						
S-B17		Y	I				
S-B17C*10		Y	I	R	Y		
S-B17D14		Y	I			F	°

[a]A circle indicates a silent mutation.

catalytic efficiency with *R*-**2** (Table SI3 of the Supporting Information). A similar behavior was also observed in the hydrolysis of epoxide **3**, albeit to a lesser degree. The *E* value for *S*,*S*-**3** increased from 84 to >1300 for variant R-C1B1D33E6, whereas the activity with *R*,*R*-**3** was below the detection limit. Clearly, the mutations introduced at L266 in the E3 and E6 variants had a negative impact on the catalytic efficiencies with both phenyl-substituted epoxides **2** and **3**.

S-4 Selected Variants. The wild-type enzyme displays an *E* value for *S*-**1** of 2.5, which was increased to approximately 6 for the furthest improved variant, S-B17D14. As for the *R*-**4** selected mutants, the K_M for both substrate enantiomers was increased (2−4-fold), which was accompanied by decreases in k_{cat} that were larger with the nonselected *R*-epoxide (Table SI3 of the Supporting Information). The observed increase in the enantiomer excess of *S*-**4** could be linked to the steady state kinetic parameters, here leading toward kinetic resolution of the *S*-**4** enantiomer.

The hydrolysis of epoxide **2** by the *S*-**4** selected variants was not substantially different from that of the wild-type enzyme, albeit with 5−10-fold lower activities for both enantiomers. A 3-fold increase in *E* for *S*-**2** was displayed by variant S-B17D14, mainly caused by a more pronounced decrease in activity with *R*-**2**.

In the reaction with epoxide **3**, the *S*-**4** selected variants displayed 15−30-fold increases in *E* for *S*,*S*-**3**. Variants S-B17C*10 and S-B17D14 both exhibited turnover numbers for *S*,*S*-**3** that exceeded that of the wild-type enzyme, while the catalytic efficiencies with the *R*,*R*-enantiomer were 70−140-fold decreased. The resulting *E* values were between 1300 and 2700 (Table SI3 of the Supporting Information).

Regioselectivity in Epoxide Ring Opening. StEH1 displays a strong preference for nucleophilic attack at C-2 in the catalyzed epoxide ring opening of both enantiomers of **1** (Figure 4 and Table SI3 of the Supporting Information). For phenyl-substituted epoxides **2** and **3**, the *S*- and *S*,*S*-enantiomers are specifically reacting at the benzylic carbon (C-1). The *R*-**2** epoxide, however, reacts primarily at the least hindered C-2, and *R*,*R*-**3** is hydrolyzed via ring opening at either carbon, with a slight preference for the benzylic carbon.

Analysis of the isolated mutants underlined the plasticity of regioselectivity. The results are summarized in Figure 4 and described below.

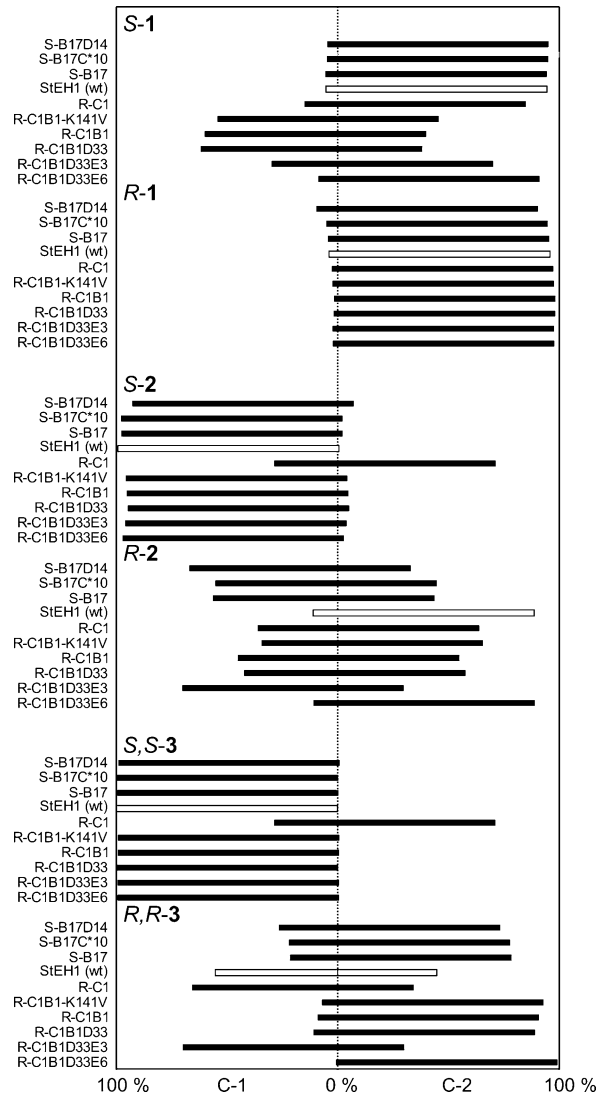

Figure 4. Regiopreferences in nucleophilic attack of the epoxide carbons of StEH1 and isolated variants. See Chart 1 for number designation.

R-4 Selected Variants. These mutants mimicked the regiopreference of the wild-type enzyme with epoxide *R*-**1**, *S*-**2**, and *S*,*S*-**3** with one exception, mutant R-C1 (V141K, I155V),

dx.doi.org/10.1021/bi3007725 | *Biochemistry* 2012, 51, 7627−7637

displaying distinct regioselectivity with both *S*-**2** and *S*,*S*-**3**. The original strong preference for attack at the benzylic carbon had been shifted to a 70:30 preference for ring opening at C-2. With epoxide *S*-**1**, the regiopreference was slightly shifted toward attack at C-1. This shift was accentuated in later generation variants R-C1B1 and R-C1B1D33. Mutations at position 266, however, reverted the regioselectivity back to attack at C-2; both E library variants R-C1B1D33E3 and R-C1B1D33E6 displayed a stronger preference for reaction at the least hindered epoxide carbon, with R-C1B1D33E6 being highly selective for attack at C-2. The shift in regioselectivity displayed by mutants R-C1B1 and R-C1B1D33, and the increased *E* values for *R*-**1** in the E library mutants, could be linked to the observed increases in *R*-**4**:*S*-**4** product ratios.

The V141K mutation found in R-C1B1 was originally seen as an accepted, but phenotypically silent, mutation because of the polar character of the side chain ammonium group that stood out in an otherwise hydrophobic active site. The regioselectivity of the R-C1B1-K141V revertant, however, displayed a lower degree of attack at C-1, resulting in a lower enantiomer excess of the *R*-diol product, demonstrating a role for K141 in steering regiopreference.

For the *R*-enantiomer of styrene oxide, the wild-type preference for attack at the least hindered C-2 was shifted toward higher degrees of reaction at the benzylic carbon, even though all variants, except R-C1B1D33E6, displayed promiscuity in regioselectivity. With *R*,*R*-**3**, the initial (slight) preference for attack at the benzylic carbon was altered to a selective reaction at C-2 in several mutants. The involvement of position 266 for steering regioselectivity in this series of variants, for both *R*-**2** and *R*,*R*-**3**, is clear from a comparison of the E library variants; R-C1B1D33E3, which contains an L266F replacement, preferentially reacts at the benzylic carbon (70:30), whereas the corresponding Gly substitution directs epoxide ring opening to occur exclusively at C-2. It should, however, be kept in mind that the overall enzymatic activity with *R*,*R*-**3** is comparably very small versus that with the *S*,*S*-enantiomer.

S-4 Selected Variants. These enzymes displayed unaltered regiopreferences with both enantiomers of **1**, *S*-**2**, and *S*,*S*-**3**. With *R*-**2**, all displayed a relaxed regioselectivity with approximately equal degrees of reaction at either epoxide carbon. The behavior with *R*,*R*-**3** was similar to that of the R variants (Figure 4), with a shift in regiopreference from C-1 to C-2 (75% C-2). Again, the actual enzyme activities with this epoxide were humbled by the corresponding activities with the *S*,*S*-enantiomer.

DISCUSSION

Manipulating Stereoselectivity in Epoxide Hydrolase. Productive enzyme engineering by rational approaches is dependent on a detailed understanding of structure–function relationships, including substrate–enzyme complementarity, dynamics, and electrostatics during the catalytic cycle. When considering fine-tuning of substrate selectivity, such as enantio- and/or regioselectivity in transformation of chiral substrates, the issue becomes even more challenging because of the relatively small differences in energy barriers. Such systems are nontrivial to describe with confidence using current theoretical methods[38] but may be approached by extensive sampling methods.[51] Hence, experimental data are dearly needed to improve our present theoretical models of stereoselectivity in these enzymes.

The main goals of this study were (i) to test the influence of changes in enantioselectivity versus regioselectivity on the outcome of the chirality of the product diols, (ii) to analyze how a structure–function trajectory generated through a pathway of stepwise mutagenesis in combination with defined selection criteria, in this case product configuration after hydrolysis of epoxide **1**, would be expressed also in reactions with other related epoxides, and (iii) to map the enzyme active site for determinants of stereoselectivity in hydrolysis of epoxides **1**–**3**.

Structure–Activity Relationships. The mutated residues were selected on the basis of their structural contributions to the active-site pocket and anticipated interactions with substrate and reaction intermediates. Although the same general approach of targeting mutation sites was applied with the *A. niger* enzyme, the altered positions in the respective active sites are in all cases different, as judged by structure alignments. For a comparison with other naturally occurring plant enzymes, sequence alignments were conducted to evaluate the variability in positions corresponding to those chosen for ISM of StEH1 (Figure SI3 of the Supporting Information). F33, which was mutated to generate A library variants, and W106, which contributes to the B libraries, are both fully conserved in these 19 plant epoxide hydrolase sequences. The reason for this strict conservation may lie in their roles in contributing their peptide backbone amides to the oxyanion hole stabilizing the negatively charged tetrahedral intermediate occurring in the hydrolytic half-reaction of catalysis. Although these interactions do not involve side chain functionalities, the conservation may reflect strict structural constraints for this stabilizing function. F33 was also strongly conserved from insertion of silent mutations in the isolated variants in this study. Although several mutants that were catalytically active were isolated, these did not display substantially improved enantiomeric excesses of the different diol **4** enantiomers and were therefore discarded from further evolution efforts.

The NDT codon set does not include a Trp codon leading to W106 being by default mutated in the library variants. From the mutants isolated and characterized, however, no evidence of special importance of the indole side chain at this position could be established; insertion of Gly, Leu, Phe, or Tyr, instead of Trp, generated functional StEH1 variants. An additional observation of the nonessential role of W106 in catalysis was made with mutant S-B16 that had retained W106, because of an artifact in the library construction. This mutant can be viewed as an F106W revertant of mutant S-B9. The ability of this single mutant to produce *S*-**4** from racemic **1** was poorer than that of the double mutant, illustrating that the absence of Trp codons in the NDT codon set did, in this case, not present limitations to the available structure–function space. This residue adjacent to the nucleophile, however, appears to be important in steering stereoselectivity because both enantio- and regiopreferences are affected by mutations at this site. This is further supported by a study in which the corresponding position in the isoenzyme from *Agrobacterium radiobacter* was mutated, resulting in variants with altered enantioselectivities.[52]

Naturally occurring substitutions found in the other corresponding mutated sites are primarily conservative and consist of nonpolar residues. One exception is V141 that in the majority of these related proteins is substituted with Pro. However, V141 is located in a loop preceding an α-helix in the lid region of the protein structure,[28] and a Pro replacement may

dx.doi.org/10.1021/bi3007725 | *Biochemistry* 2012, 51, 7627–7637

therefore also, by virtue of the nonpolar nature of this residue, be considered as conservative.

Regio- and Enantioselectivities Affecting Product Ratios. Regioselectivity in the StEH1-catalyzed hydrolysis of phenyl-substituted epoxides is apparently plastic[32,33] and is expected to depend on structural constraints for the formation of a productive ES complex promoting nucleophilic attack at a reactive carbon. In cases where the enzyme displays promiscuity in regiopreference, two diol products will be formed at ratios determined by the flux through the different reaction pathways (Scheme 2).

Scheme 2. Model of StEH1-Catalyzed Hydrolysis of Epoxides

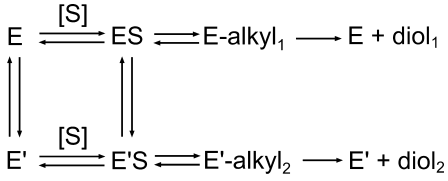

The validity of the model in Scheme 2 has been demonstrated previously.[33] The model accounts for all cases of varying degrees of regioselectivity and also explains the hysteretic behavior that is frequently observed with this enzyme, such as the sigmoid substrate concentration dependence of initial velocities. Several variants isolated in this study displayed tendencies of cooperative substrate dependency, although not to the extent that addition of extra parameters to the Michaelis–Menten equation was significantly justified. This observation, however, emphasizes that in a complex kinetic mechanism, such as this, mutations introduced when moving through evolutionary trajectories should be expected to shift the flux through the different branches of the pathway and thereby also affect the product ratios.

For several enzyme variants in this study, showing improved preferences for formation of either of the products *S*- or *R*-**4**, only modest increases in *E* values were obtained. This was puzzling, but the explanation could be traced to alterations in regioselectivity. Consequently, if there is a change in regioselectivity, or a tendency of promiscuity, considering strictly the *E* values of an enzyme variant would not reveal the full story. This was exemplified by the *R*-**4** selected variants R-C1B1, R-C1B1-K141V, and R-C1B1D33 with a significant change, from attack at C-2, for wild-type StEH1, to a preferred attack at C-1, with epoxide *S*-**1** (Figure 4). This, in combination with an unaltered (strict) regioselectivity toward C-2 for *R*-**1**, led to a higher percentage of *R*-**4** than otherwise expected from the *E* values alone. The resulting enantioconvergence is a desired property because the limiting yield of enantiopure product of 50% from a kinetic resolution of a racemic substrate can be exceeded. This phenomenon of enantioconvergence has previously been successfully demonstrated for an epoxide hydrolase from *A. niger*, using a related substrate.[53]

In the formulation of a possible mechanism for the observed effects on enantio- and regioselectivities of the evolved StEH1 mutants, the concept of structural dynamism[54] is fitting. This model assumes the existence of an ensemble of protein conformations with a given equilibrium distribution where different conformers possess distinct functional properties, as is also suggested by Scheme 2. Mutations in the protein and/or subjection to nonphysiological substrates, in the case of enzymes, may shift the equilibria toward conformations allowing functionalities different from that of the original wild type. Hence, the described StEH1 variants may accordingly display distinct conformer distributions compared to the wild type, reflected in their acquired functional properties. The R-C1 variant has accumulated two mutations, V141K and I155V. This mutant displays special regioselectivities with the *S*- and *S*,*S*-enantiomers of styrene oxide and methylstyrene oxide, respectively (Figure 4). This feature was a nonselected for property, silent during the selection process that targeted improved formation of *R*-**4**, but illustrates that also minor structural changes can result in substantial effects. In the second- and third-generation mutants originating from R-C1, this unexpected behavior reverted back to the initial selectivity, concomitant with a shift in regiopreference from C-2 to C-1 in the ring-opening reaction with *S*-**1**. Therefore, it appears that intrinsic preexisting potentials of different regiopreferences and catalytic efficiencies are disclosed by mutagenesis and/or the presence of a particular substrate, e.g., styrene oxide, in this case.

Because of the lack of detailed structural data for the isolated mutants, attempts to link the observed regiopreferences of these variants with the structural alterations would become speculative. The difference in energy barriers between attack at C-1 or C-2 can be calculated from the relative ratios of reacting epoxide carbon [$\Delta\Delta G = -RT \ln(\text{C-1/C-2})$]. In the case of wild-type StEH1, displaying 93% attack at C-2 of *S*-**1** (Table SI3 of the Supporting Information), the energy difference is +6.5 kJ/mol. In mutant R-C1B1, the same difference is only −1 kJ/mol, so the introduced mutations account for a total change of <8 kJ/mol in changing the regiopreference from C-2 to C-1. The structural changes that contribute to the major shift are W106L and L109Y. W106 fulfills dual roles in the catalysis by StEH1: it contributes via the main chain amide to the oxyanion hole stabilizing the tetrahedral intermediate that is formed during the hydrolytic half-reaction of catalysis, and through its indole side chain to substrate interactions. L109, situated one α-helix turn from W106 (Figure 1), likewise contributes its side chain for substrate interactions. Via comparison of the regiopreferences of mutants R-C1B1 and S-B17, it is noteworthy that retaining an aromatic residue at position 106 also preserves the regioselectivity of the wild-type enzyme in the reaction with *S*-**1**.

The shift in regiopreferences from C-2 to C-1 for mutant R-C1B1 (and R-C1B1D33) reverts in the next-generation E library variants, R-C1B1D33E3 and -E6 (Figure 4 and Table SI3 of the Supporting Information). Both these variants are single mutants, L266F and L266G, respectively, of the parent. In the wild-type enzyme, the side chain C-δ atom of L266 is 3.8 Å from both the phenolic hydroxyl of Y154 and the ε-2 carbon of the F189 phenyl ring. In variant R-C1B1D33 and its offspring, F189 is replaced with Leu, introducing more space in this region of the active site. With this in mind, the observed effects on the regiopreferences in mutants R-C1B1D33E3 and -E6 are puzzling; in the L266F variant, the introduction of the benzyl substituent is expected to create a clash with the side chain of Y154 and cause local rearrangements of these residues. Such rearrangements may affect the hydrogen bonding with the substrate epoxide oxygen and/or the stabilization of the alkyl–enzyme intermediate causing a shift in the regiopreference. In the E6 mutant, however, L266 is replaced with Gly, thus removing all side chain bulk. Possibly, also an increased accessible volume in the active-site cavity may result in local

dx.doi.org/10.1021/bi3007725 | *Biochemistry* 2012, 51, 7627–7637

rearrangements of the catalytic Y154 with similar end results in the observed regiopreferences. In a recent theoretical study of stereoselectivity of the murine soluble epoxide hydrolase, the importance of hydrogen bonding between the active-site tyrosines and the epoxide oxygen was emphasized.[38]

Improved enantioselectivity of an evolved enzyme may arrive at the cost of a decrease in catalytic activity, and a high enantiomeric excess might not be practically significant if it sacrifices high catalytic efficiency. It is therefore important to also include information describing, e.g., product formation, which has been done in Figure 5. Upon comparison of the

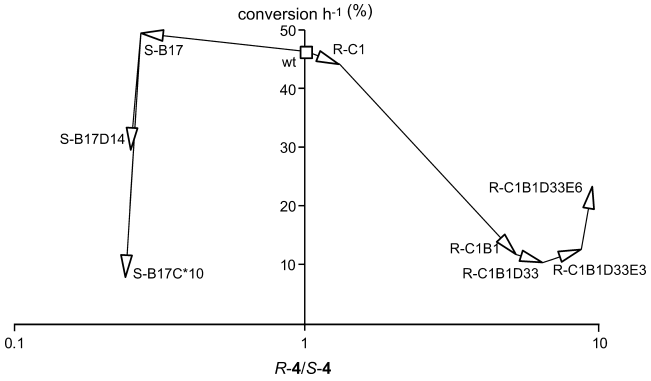

Figure 5. Evolution of conversion of *rac*-**1** into either *S*-**4** (left) or *R*-**4** (right) as a function of *R*-**4**:*S*-**4** product ratios during ISM. *rac*-**1** (30.4 mM) was incubated with 0.5 μM StEH1 variant enzymes for 1 h.

resulting diol production from racemic epoxide mixtures with product outcomes calculated from kinetic data of reactions with pure enantiomers (see Table SI3 of the Supporting Information), certain differences are observed. The kinetics of racemate hydrolysis is more complex, and simulations taking into account only the kinetic parameters for each of the pure enantiomers therefore result in misleading results. This is probably due to trivial issues of one enantiomer acting as an inhibitor of the other and/or product inhibition. For the reactions shown in Figure 5, the maximal conversion is 50% if strict regioselectivity is assumed. This means that in the reactions with wild-type StEH1 and the S-B17 variant, all substrates have been consumed. It should also be pointed out that it is possible to regain enzyme activity while moving along the evolutionary trajectory, as indicated by the R variants where R-C1B1D33E6 displays 25% conversion per hour.

CONCLUSIONS

The iterative saturation mutagenesis approach as applied to StEH1 allowed isolation of new epoxide hydrolase variants producing enriched fractions of diol *R*-**4** or, albeit to a lesser extent, diol *S*-**4** from a racemic epoxide starting material. The increased product purities were due to increased *E* values for the corresponding substrate enantiomer(s) or in combination with a change in the regiopreference of the initial enzyme afforded epoxide ring opening. A number of variants also displayed altered catalytic properties with epoxide **2** or **3** as exemplified by R-C1B1D33, showing an *E* value for *S*-**2** that increased from 69 to 5800. Thus, the libraries that we constructed showed potential of being applicable for a broader substrate range than was initially screened for. Although detailed structural data of the isolated mutants, supported by theoretical studies, are needed to link the observed functional properties with the structural alterations, the functional data presented here suggest that the amino acid residue positioned C-terminally and adjacent to the nucleophile influences stereoselectivity in these reactions.

ASSOCIATED CONTENT

Supporting Information

Tables and figures with details of results from NMR analysis, sequence alignments, library constructions and characterization, and enzyme kinetics. This material is available free of charge via the Internet at http://pubs.acs.org.

AUTHOR INFORMATION

Corresponding Author

*E-mail: mikael.widersten@kemi.uu.se. Phone: +46 (0)18 471 4992.

Funding

The work was supported by the Swedish Research Council (Grants VR 621-2008-3579 and 621-2011-6055).

Notes

The authors declare no competing financial interest.

ACKNOWLEDGMENTS

We thank Prof. Adolf Gogoll for assistance with the NMR analysis, Dr. M. Stieger (F. Hoffmann-La Roche, Basel, Switzerland) for providing the pREP4 GroEL/ES plasmid, and Dr. Lynn Kamerlin for manuscript review.

REFERENCES

(1) Bornschauer, U. T., Huisman, G. W., Kazlauskas, R. J., Lutz, S., Moore, J. C., and Robins, K. (2012) Engineering the third wave of biocatalysis. *Nature 485*, 185−194.

(2) Chen, K., and Arnold, F. H. (1991) Enzyme engineering for nonaqueous solvents: Random mutagenesis to enhance activity of subtilisin E in polar organic media. *Nat. Biotechnol. 9*, 1073−1077.

(3) Chen, K., Robinson, A. C., Van Dam, M. E., Martinez, P., Economou, C., and Arnold, F. H. (1991) Enzyme engineering for nonaqueous solvents. II. Additive effects of mutations on the stability and activity of subtilisin E in polar organic media. *Biotechnol. Prog. 7*, 125−129.

(4) Chartrain, M., Salmon, P. M., Robinson, D. K., and Buckland, B. C. (2000) Metabolic engineering and directed evolution for the production of pharmaceuticals. *Curr. Opin. Biotechnol. 11*, 209−214.

(5) Hult, K., and Berglund, P. (2003) Engineered enzymes for improved organic synthesis. *Curr. Opin. Biotechnol. 14*, 395−400.

(6) Reetz, M. T., Bocola, M., Carballeira, J. D., Zha, D., and Vogel, A. (2005) Expanding the range of substrate acceptance of enzymes: Combinatorial active-site saturation test. *Angew. Chem., Int. Ed. 44*, 4192−4196.

(7) Turner, N. J. (2009) Directed evolution drives the next generation of biocatalysts. *Nat. Chem. Biol. 5*, 567−573.

(8) Clouthier, C. M., and Pelletier, J. N. (2012) Expanding the organic toolbox: A guide to integrating biocatalysis in synthesis. *Chem. Soc. Rev. 41*, 1585−1605.

(9) Harris, J. L., and Craik, C. S. (1998) Engineering enzyme specificity. *Curr. Opin. Chem. Biol. 2*, 127−l32.

(10) Bloom, J. D., Meyer, M. M., Meinhold, P., Otey, C. R., MacMillan, D., and Arnold, F. H. (2005) Evolving strategies for enzyme engineering. *Curr. Opin. Struct. Biol. 15*, 447−452.

(11) Chica, R. A., Doucet, N., and Pelletier, J. N. (2005) Semi-rational approaches to engineering enzyme activity: Combining the benefits of directed evolution and rational design. *Curr. Opin. Biotechnol. 16*, 378−384.

(12) Kaur, J., and Sharma, R. (2006) Directed evolution: An approach to engineer enzymes. *Crit. Rev. Biotechnol. 26*, 165−199.

(13) Kirschner, A., and Bornscheuer, U. T. (2008) Directed evolution of a Baeyer-Villiger monooxygenase to enhance enantioselectivity. *Appl. Microbiol. Biotechnol. 81*, 465−472.
(14) Larrow, J. F., and Jacobsen, E. N. (2004) Assymetric processes catalyzed by chiral (salen) metal complexes. *Top. Organomet. Chem. 6*, 123−152.
(15) Lacourciere, G. M., and Armstrong, R. N. (1993) The catalytic mechanism of microsomal epoxide hydrolase involves an ester intermediate. *J. Am. Chem. Soc. 115*, 10466−10467.
(16) Borhan, B., Jones, A. D., Pinot, F., Grant, D. F., Kurth, M. J., and Hammock, B. D. (1995) Mechanism of soluble epoxide hydrolase. Formation of an α-hydroxy ester-enzyme intermediate through Asp-333. *J. Biol. Chem. 270*, 26923−26930.
(17) Pinot, F., Grant, D. F., Beetham, J. K., Parker, A. G., Borhan, B., Landt, S., Jones, A. D., and Hammock, B. D. (1995) Molecular and biochemical evidence for the involvement of the Asp-333-His-523 pair in the catalytic mechanism of soluble epoxide hydrolase. *J. Biol. Chem. 270*, 7968−7974.
(18) Tzeng, H.-F., Laughlin, T. L., Lin, S., and Armstrong, R. N. (1996) The catalytic mechanism of microsomal epoxide hydrolase involves reversible formation and rate-limiting hydrolysis of the alkyl−enzyme intermediate. *J. Am. Chem. Soc. 118*, 9436−9437.
(19) Arand, M., Cronin, A., Oesch, F., Mowbray, S. L., and Jones, T. A. (2003) The telltale structures of epoxide hydrolases. *Drug Metab. Rev. 35*, 365−383.
(20) Arand, M., Cronin, A., Adamska, M., and Oesch, F. (2005) Epoxide hydrolases: Structure, function, mechanism, and assay. *Methods Enzymol. 400*, 569−588.
(21) Morisseau, C., and Hammock, B. D. (2005) Epoxide hydrolases: Mechanisms, inhibitor designs, and biological roles. *Annu. Rev. Pharmacol. Toxicol. 45*, 311−333.
(22) Widersten, M., Gurell, A., and Lindberg, D. (2010) Structure-function relationships of epoxide hydrolases and their potential use in biocatalysis. *Biochim. Biophys. Acta 1800*, 316−326.
(23) Rink, R., Kingma, J., Lutje Spelberg, J. H., and Janssen, D. B. (2000) Tyrosine residues serve as proton donor in the catalytic mechanism of epoxide hydrolase from *Agrobacterium radiobacter*. *Biochemistry 39*, 5600−5613.
(24) Elfström, L. T., and Widersten, M. (2006) Implications for an ionized alkyl-enzyme intermediate during StEH1-catalyzed *trans*-stilbene oxide hydrolysis. *Biochemistry 45*, 205−212.
(25) Stapleton, A., Beetham, J. K., Pinot, F., Garbarino, J. E., Rockhold, D. R., Friedman, M., Hammock, B. D., and Belknap, W. R. (1994) Cloning and expression of soluble epoxide hydrolase from potato. *Plant J. 6*, 251−258.
(26) Elfström, L. T., and Widersten, M. (2005) Catalysis of potato epoxide hydrolase, StEH1. *Biochem. J. 390*, 633−640.
(27) Gurell, A., and Widersten, M. (2010) Modification of substrate specificity resulting in an epoxide hydrolase with shifted enantiopreference for (2,3-epoxypropyl)benzene. *ChemBioChem 11*, 1422−1429.
(28) Mowbray, S. L., Elfström, L. T., Ahlgren, K. M., Andersson, C. E., and Widersten, M. (2006) X-ray structure of potato epoxide hydrolase sheds light on substrate specificity in plant enzymes. *Protein Sci. 15*, 1628−1637.
(29) Reetz, M. T., Wang, L.-W., and Bocola, M. (2006) Directed evolution of enantioselective enzymes: Iterative cycles of CASTing for probing protein-sequence space. *Angew. Chem., Int. Ed. 45*, 1236−1241.
(30) Reetz, M. T., Bocola, M., Wang, L.-W., Sanchis, J., Cronin, A., Arand, M., Zou, J., Archelas, A., Bottalla, A.-L., Naworyta, A., and Mowbray, S. L. (2009) Directed evolution of an enantioselective epoxide hydrolase: Uncovering the source of enantioselectivity at each evolutionary stage. *J. Am. Chem. Soc. 131*, 7334−7343.
(31) Parker, R. E., and Isaacs, N. S. (1959) Mechanisms of epoxide reactions. *Chem. Rev. 59*, 737−799.
(32) Monterde, M. I., Lombard, M., Archelas, A., Cronin, A., Arand, M., and Furstoss, R. (2004) Enzymatic transformations. Part 58: Enantioconvergent biohydrolysis of styrene oxide derivatives catalysed by the *Solanum tuberosum* epoxide hydrolase. *Tetrahedron: Asymmetry 15*, 2801−2805.
(33) Lindberg, D., de la Fuente Revenga, M., and Widersten, M. (2010) Temperature and pH dependence of enzyme catalyzed hydrolysis of *trans*-methylstyrene oxide: A unifying kinetic model for observed hysteresis, cooperativity and regioselectivity. *Biochemistry 49*, 2297−2304.
(34) Thomaeus, A., Carlsson, J., Åqvist, J., and Widersten, M. (2007) Active site of epoxide hydrolases revisited: A noncanonical residue in potato StEH1 promotes both formation and breakdown of the alkylenzyme intermediate. *Biochemistry 46*, 2466−2479.
(35) Lau, E. Y., Newby, Z. E., and Bruice, T. C. (2001) A theoretical examination of the acid-catalyzed and noncatalyzed ring-opening reaction of an oxirane by nucleophilic addition of acetate. Implications to epoxide hydrolases. *J. Am. Chem. Soc. 123*, 3350−3357.
(36) Schiøtt, B., and Bruice, T. C. (2002) Reaction mechanism of soluble epoxide hydrolase: Insights from molecular dynamics simulations. *J. Am. Chem. Soc. 124*, 14558−14570.
(37) Hopmann, K. H., and Himo, F. (2006) Theoretical study of the full reaction mechanism of human soluble epoxide hydrolase. *Chemistry 12*, 6898−6909.
(38) Lonsdale, R., Hoyle, S., Grey, D. T., Ridder, L., and Mulholland, A. D. (2012) Determinants of reactivity and selectivity in soluble epoxide hydrolases from quantum mechanics/molecular mechanics modeling. *Biochemistry 51*, 1774−1786.
(39) Reetz, M. T., and Carballeira, J. D. (2007) Iterative saturation mutagenesis (ISM) for rapid directed evolution of functional enzymes. *Nat. Protoc. 2*, 891−903.
(40) Reetz, M. T., Prasad, S., Carballeira., J. D., Gumulya, Y., and Bocola, M. (2010) Iterative saturation mutagenesis accelerates laboratory evolution of enzyme stereoselectivity: Rigorous comparison with traditional methods. *J. Am. Chem. Soc. 132*, 9144−9152.
(41) Reetz, M. T., Carballeira, J. D., and Vogel, A. (2006) Iterative saturation mutagenesis on the basis of B factors as a strategy for increasing protein thermostability. *Angew. Chem., Int. Ed. 45*, 7745−7751.
(42) Bougioukou, D. J., Kille, S., Taglieber, A., and Reetz, M. T. (2009) Directed evolution of an enantioselective enoate-reductase: Testing the utility of iterative saturation mutagenesis. *Adv. Synth. Catal. 351*, 3287−3305.
(43) Zheng, H., and Reetz, M. T. (2010) Manipulating the stereoselectivity of limonene epoxide hydrolase by directed evolution based on iterative saturation mutagenesis. *J. Am. Chem. Soc. 132*, 15744−15751.
(44) Engström, K., Nyhlén, J., Sandström, A. G., and Bäckvall, J.-E. (2010) Directed evolution of an enantioselective lipase with broad substrate scope for hydrolysis of α-substituted esters. *J. Am. Chem. Soc. 132*, 7038−7042.
(45) Prasad, S., Bocola, M., and Reetz, M. T. (2011) Revisiting the lipase from *Pseudomonas aeruginosa*: Directed evolution of substrate acceptance and enantioselectivity using iterative saturation mutagenesis. *ChemPhysChem 12*, 1550−1557.
(46) Reetz, M. T., Kahakeaw, D., and Lohmer, R. (2008) Addressing the numbers problem in directed evolution. *ChemBioChem 9*, 1797−1804.
(47) Dale, G. E., Schönfeld, H. J., Langen, H., and Stieger, M. (1994) Increased solubility of trimethoprim-resistant type S1 DHFR from *Staphylococcus aureus* in *Escherichia coli* cells overproducing the chaperonins GroEL and GroES. *Protein Eng. 7*, 925−931.
(48) Agarwal, S. C., Van Duuren, B. L., and Kneip, T. J. (1979) Detection of epoxides with 4-(*p*-nitrobenzyl) pyridine. *Bull. Environ. Contam. Toxicol. 23*, 825−829.
(49) Altschul, S. F., Gish, W., Miller, W., Myers, E. W., and Lipman, D. J. (1990) Basic local alignment search tool. *J. Mol. Biol. 215*, 403−410.
(50) Thompson, J. D., Higgins, D. G., and Gibson, T. J. (1994) CLUSTAL W: Improving the sensitivity of progressive multiple sequence alignment through sequence weighting, position specific gap penalties and weight matrix choice. *Nucleic Acids Res. 22*, 4673−4680.

(51) Frushicheva, M. P., and Warshel, A. (2012) Towards quantitative computer-aided studies of enzymatic enantioselectivity: The case of *Candida antarctica* lipase A. *ChemBioChem 13*, 215−223.
(52) Van Loo, B., Kingma, J., Heyman, G., Wittenaar, A., Lutje Spelberg, J. H., Sonke, T., and Janssen, D. B. (2009) Improved enantioselective conversion of styrene epoxides and *meso*-epoxides through epoxide hydrolases with a mutated nucleophile-flanking residue. *Enzyme Microb. Technol. 44*, 145−153.
(53) Zheng, H., Kahakeaw, D., Acevedo, J. P., and Reetz, M. T. (2010) Directed evolution of enantioconvergency: The case of an epoxide hydrolase-catalyzed reaction of a racemic epoxide. *ChemCatChem 2*, 958−961.
(54) Tokuriki, N., and Tawfik, D. S. (2009) Protein dynamism and evolvability. *Science 324*, 203−207.